The K2 Bright Star Survey

Benjamin J. S. Pope,[1, 2, 3] Timothy R. White,[4] Conny Aerts,[5, 6]
Suzanne Aigrain,[7] Timothy R. Bedding,[8, 9] Tabetha Boyajian,[10]
Orlagh L. Creevey,[11] Will M. Farr,[12, 13] David W. Hogg,[1, 2, 14, 15]
Daniel Huber,[16, 17, 9] and friends

[1]*Center for Cosmology and Particle Physics, Department of Physics, New York University, 726 Broadway, New York, NY 10003, USA*

[2]*Center for Data Science, New York University, 60 Fifth Ave, New York, NY 10011, USA*

[3]*NASA Sagan Fellow*

[4]*Research School of Astronomy and Astrophysics, Mount Stromlo Observatory, The Australian National University, Canberra, ACT 2611, Australia*

[5]*Instituut voor Sterrenkunde, KU Leuven, Celestijnenlaan 200D, B-3001 Leuven, Belgium*

[6]*Department of Astrophysics, IMAPP, Radboud University Nijmegen, P.O. Box 9010, NL-6500 GL Nijmegen, The Netherlands*

[7]*Oxford Astrophysics, Denys Wilkinson Building, University of Oxford, OX1 3RH, Oxford, UK*

[8]*Sydney Institute for Astronomy, School of Physics A28, The University of Sydney, NSW 2006, Australia*

[9]*Stellar Astrophysics Centre, Department of Physics and Astronomy, Aarhus University, DK-8000 Aarhus C, Denmark*

[10]*Department of Physics and Astronomy, Louisiana State University, 202 Nicholsom Hall, Baton Rouge, LA 70803, USA*

[11]*Université Côte d'Azur, Observatoire de la Côte d'Azur, CNRS, Laboratoire Lagrange, Bd de l'Observatoire, CS 34229, 06304 Nice cedex 4, France*

[12]*Center for Computational Astrophysics, Flatiron Institute, 162 Fifth Ave, New York, NY 10010, USA*

[13]*Department of Physics and Astronomy, Stony Brook University, Stony Brook, NY 11794, USA*

[14]*Max-Planck-Institut für Astronomie, Königstuhl 17, D-69117 Heidelberg*

[15]*Flatiron Institute, 162 Fifth Ave, New York, NY 10010, USA*

[16]*Institute for Astronomy, University of Hawai'i, 2680 Woodlawn Drive, Honolulu, HI 96822, USA*

[17]*SETI Institute, 189 Bernardo Avenue, Mountain View, CA 94043, USA*

ABSTRACT

While the *Kepler* Mission was designed to look at tens of thousands of faint stars ($V \gtrsim 12$), brighter stars, which saturate the detector, are important because they can be and have been observed by other instruments at very high signal-to-noise ratio. By considering the unsaturated scattered light 'halo' around these stars we can and do retrieve precise light curves of most of the brightest stars in *K2* fields from Campaign 4

Corresponding author: Benjamin J. S. Pope 🐦 @fringetracker
benjamin.pope@nyu.edu

onwards. The halo method is highly agnostic about the cause and form of systematics and we show that it nevertheless it is effective at extracting light curves from both normal and saturated stars. The key methodology is to optimize the weights of a linear combination of pixel time series with respect to an objective function. We test a range of such objective functions, finding that generalizations of Total Variation perform well on both saturated and unsaturated *K2* targets. Applying this to the bright stars across the *K2* Campaigns, this reveals stellar variability ubiquitously, including effects of stellar pulsation, rotation, and binarity. Here we describe our pipeline, and present a catalogue of the bright stars studied, with classifications and parametrizations of their variability and remarks on interesting objects. These light curves are publicly available as a High Level Science Product from the Mikulski Archive for Space Telescopes (MAST). ⃝

1. INTRODUCTION

The *Kepler* Space Telescope was launched with a main goal of determining the frequency of Earth-sized planets around Solar-like stars (Borucki et al. 2010), a goal which it has substantially achieved (e.g. Fressin et al. 2013; Petigura et al. 2013; Foreman-Mackey et al. 2014). In order to explore these populations it was necessary to observe hundreds of thousands of stars, with the consequence that the *Kepler* the exposure time and gain were set to optimally observe eleventh or twelfth-magnitude stars, while bright stars are saturated and these saturated stars were intentionally avoided. In the two-wheeled revival as the *K2* mission, the *Kepler* telescope observed a sequence of ecliptic-plane fields containing many more very-saturated stars. While it is difficult to obtain precise light curves of these stars because of their saturation, they are some of the most-valuable targets to follow up with photon-hungry methods such as interferometry or high-resolution spectroscopy, and they typically have long histories of previous observations.

The *Kepler* detector saturates at a magnitude of $K_p \sim 11.3$ in both long- (30 min) and short (1 min)-cadence data, as these both represent sums of 6 s exposures (Gilliland et al. 2010). For objects brighter than this, additional photons create excess electrons which 'bleed' into adjacent pixels in both directions along the column containing the bright star. Simple aperture photometry (SAP) – adding all the flux contained in a window around the bleed column – has recovered light curves with precisions close to the photon noise limit of stars as bright as 16 Cyg AB, θ Cyg and RR Lyr (e.g. Kolenberg et al. 2011; White et al. 2013; Guzik et al. 2016). In the nominal *Kepler* mission this was not attempted for all such bright stars, and in *K2* , the several-pixel spacecraft motion significantly increased the size of the required apertures for SAP photometry of very saturated stars, while also making their systematics more difficult to deal with. While the second-version pixel-level-decorrelation (PLD) pipeline EVEREST 2.0 was able to correct systematics in saturated SAP photometry (Luger et al. 2018), this is rendered impossible for the very brightest stars whose bleed

columns may run to the edge of the detector. Furthermore, bandwidth constraints meant that pixel data were not downloaded for many bright targets in *K2* .

In order to recover precise photometry of the brightest stars in *K2* , we have therefore developed two main approaches, 'smear' and 'halo' photometry. Smear photometry (Pope et al. 2016) uses collateral 'smear' calibration data to obtain a 1-D spatial profile with $\sim 1/1000$ of the flux on each CCD. This can be processed recover light curves of stars which were not necessarily conventionally targeted and downloaded with active pixels, because smear data are recorded for all columns. The main disadvantage of this method is that it confuses all stars in the same column, which means that in crowded fields smear light curves tend to be significantly contaminated.

The more precise method of halo photometry, which is the subject of this paper, uses the broad 'halo' of scattered light around a saturated star to recover relative photometry, by constructing a light curve as a linear combination of individual pixel time series and minimizing a Total Variation objective function (TV-min). It has been employed for example on the Pleiades (White et al. 2017) and the brightest-ever star on *Kepler* silicon, Aldebaran (Farr et al. 2018), recovering photometry with a precision nearly that of normally-obtained *K2* observations of unsaturated stars. Unlike smear, this requires downloading data out to a 12–20 pixel radius around each star, and has accordingly only been possible for stars that were specifically targeted with apertures optimized for this method and for a small number of other stars for which this is fortuitously the case. The pixel requirements for this are sufficiently low that, with the help of the *K2* Guest Observer office, such apertures were obtained for most of the bright targets from Campaign 4 onwards.

In this Paper we describe numerical experiments testing the TV-min method and extending it to generalizations with different exponents and timescales. We show that the method as previously employed applying standard TV-min is suboptimal, and gain a modest improvement from taking finite differences close to the timescale of *K2* thruster firings. We go on to present complete catalog of long-cadence *K2* halo light curves, which we have made publicly available. We have employed halo photometry on all stars targeted with appropriate apertures, and have done a preliminary characterization of interesting astrophysical variability. We also document the main changes in the halo data reduction pipeline, `halophot`, with respect to previous releases. These include oscillating red giants, pulsating and quiet main sequence stars, and eclipsing binaries, many of which are among the brightest objects of their type to have been observed with space photometry. We hope that this diverse catalog of light curves will be useful for an equally-diverse range of astrophysical investigations.

2. HALO PHOTOMETRY METHOD

This method was first described by White et al. (2017) and applied to the Pleiades' Seven Sisters, and was applied to Aldebaran with further developments by Farr et al. (2018). Because SAP is not possible, we consider instead the unsaturated pixels p_j

at the wings of the broad and structured PSF. We construct a light curve as a linear combination of these time series with weights w_j, so that flux at cadence i is

$$f_i \equiv \sum_j w_j p_{ij}. \tag{1}$$

In our updated pipeline presented here, the weights are chosen to minimize an objective function

$$Q_{k,l} \equiv \sum_i |f_i - f_{i-\delta}|^k, \tag{2}$$

subject to the constraints

$$\forall_j w_j > 0 \tag{3}$$

$$\sum_{i=1}^N f_i = N. \tag{4}$$

This is a classic convex optimization program with constraints, which we solve with the `scipy` (Jones et al. 2001) L-BFGS-B nonlinear optimization code (Zhu et al. 1999). $Q_{k,l}$ has analytic derivatives with respect to w_j (calculated with `autograd`; Maclaurin et al. 2015), and it is therefore extremely fast to optimize and converges well on a global solution. In practice, for computational reasons we optimize over parameters $\tilde{w}_j$ such that $w_j = \text{softmax}(\tilde{w}_j$, as this satisfies the constraint that $\forall_j w_j > 0$, and while this also constrains their sum to be unity, we renormalize f to satisfy its normalization constraint before calculating the objective function and this additional constraint is removed again.

The objective function $Q_{k,l}$ is the L_k norm on a 'lagged' finite difference with a lag parameter δ. For $k = 1$ and $\delta = 1$, $Q_{1,1}$ is the standard Total Variation objective (TV) used in previous halo papers (e.g. White et al. 2017; Farr et al. 2018), and can be seen as the L1 norm on the derivative of f or as a discrete approximation to its arc length. The L2 Variation (L2V) with $k = 2$ is sometimes referred to in image processing literature as the 'smoothness' regularizer, as it seeks to penalize large gradients without necessarily making them sparse. The lag parameter δ allows for flexibility in modelling systematics occurring at different timescales from cadence-to-cadence, and we investigate its effects below. The order parameter k allows for flexibility in how sensitive we are to normally-distributed versus long-tailed noise. For convenience in the rest of this paper, we will refer to the $k = 1$ case as TV, the $k = 2$ case as L2V, and the $k = 3$ case as L3V.

In order to choose the values for k and δ in our objective function, we have selected the quiet star 36 Ophiuchi, the lowest-mass main sequence star in the sample of stars with halo apertures, and one with very little high frequency variability detected or predicted, which was also observed at short cadence. We choose the 6.5 hour
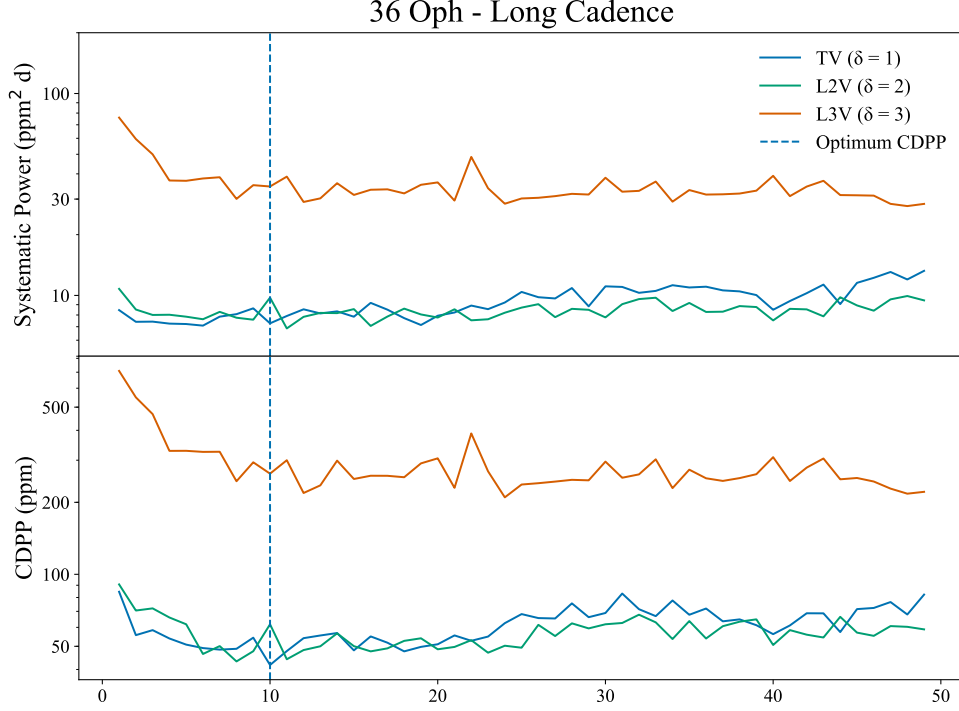
Figure 1. Behaviour of long cadence 6.5 hour CDPP (bottom) and $4c/d$ systematics power (top) for the quiet dwarf 36 Ophiuchi as a function of lag parameter δ. CDPP shows a minimum for L1 norm and $\delta = 10$, i.e. for objective function $Q_{1,10}$, which is marked with a blue dashed vertical line. This does not correspond to an optimum in systematic power, which is slightly lower for smaller δ. Nevertheless, we have chosen $\delta = 10$ for the light curves in this catalog because of its improvement in overall CDPP as a measure of planet detection efficiency and overall light curve quality.

Combined Differential Photometric Precision (CDPP, Christiansen et al. 2012) as implemented in `lightkurve` (Vinícius et al. 2018) as a proxy for the 'noise' in a lightcurve, with lower being better. We calculate halo lightcurves and their CDPPs for $k \in \{1, 2, 3\}$, and $\delta \in [1, 50]$ for long cadence and for various valies of $\delta \in [1, 2500]$ for short cadence data. The results are displayed in Figure 2. We find that for long cadence data, $k = 1$ (TV) and a lag $\delta = 10$ provide the best CDPP. This is unsurprising: that this is one cadence shorter than the 12 cadence thruster firing period. In this context we can understand the optimum as suppressing systematics on the same timescale as they occur. On the other hand, for short cadence data, performance at short lags is very poor but the method performs similarly for $k \in \{1, 2\}$ with slow improvement with larger δ, and performs very poorly for $k = 3$ at all lags.

Unlike other methods for calibrating *Kepler* systematics, other than the value of δ, no knowledge of the spacecraft motion or the behaviour of an ensemble of other stars is used to inform our algorithm. The method is a self-calibration that is independent of the details of the systematics it is calibrating, operating on the assumption that a single signal is present across many individual time series which otherwise are contaminated by noise. It is therefore likely that significant improvements can be made to
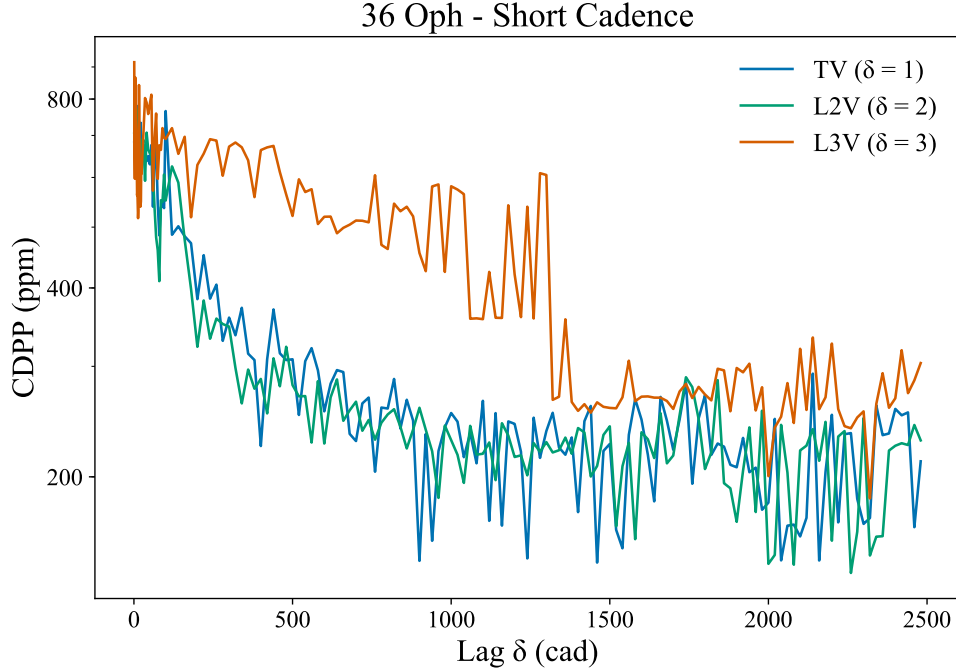
Figure 2. Behaviour of short cadence 6.5 hour CDPP for the quiet dwarf 36 Ophiuchi as a function of lag parameter δ. CDPP continuously improves for higher lags and shows no strong differences between L1 and L2 norms, while L3 performs poorly.

the method by including cotrending basis vectors with mean zero and whose weights are allowed to be negative, which would represent systematics which are common to all pixels in the halo aperture and therefore masquerade as signal. Any linear combination of convex objective functions is itself convex, and future extensions to the method could enforce combinations of different lags and orders to better represent systematics occurring on different timescales (e.g. thruster firings, red noise) and with different levels of smoothness.

In addition to expanding the range of possible objective functions, we have also added a feature '`deathstar`' to deal with contamination. We apply the watershed-based image segmentation algorithm from к2р2 (Lund et al. 2015) to the input target pixel file datacube to identify possible background sources and cut them out. More here from Tim. Other than this, we have adopted less-aggressive quality flagging, having found that many cadences were being classified as bad quality for spurious 'cosmic ray' events, which were actually caused by a combination of saturation and spacecraft motion. We now iteratively sigma-clip outliers and retain cadences with the `lightkurve` default quality mask.

While the halo procedure produces in most cases a fairly clean light curve, there are nevertheless residual systematic errors related to spacecraft motion. In order to correct these, we employ the к2sc code (Aigrain et al. 2015, 2016), which simultaneously models a light curve as a 3D Gaussian Process (GP) in time and predicted position (the K2 standard data product pos_corr) in pixels (x, y). The model prediction in

time for fixed position is then a nonparametric model of the stellar variability, and the prediction for the x, y component evaluated for fixed time represents the pointing systematics. We subtract the systmatics model from the input fluxes to obtain a final corrected flux, which is the time series we use and recommend for science. The target pixel files for C91, C92, and C101 include no position information, and there are no halo apertures for C112. As a result K2SC-corrected data are not available for these targets.

3. SAMPLE

The full sample of stars for which halo apertures were obtained is listed in Table 1. While some very bright stars were observed with conventional apertures as part of these programs, simple aperture photometry is satisfactory on these targets and we exclude them from the present discussion and data release, which is oriented strictly towards targets only observable with halo photometry. We make an exception for Spica, which was observed in Campaign 6 without a halo aperture but in Campaign 17 with a halo aperture. In Campaign 6 it was assigned a normal aperture by mistake and simple aperture photometry performed extremely poorly, so we have processed it with the halo pipeline. The stars in Campaign 18 were also on-silicon in Campaign 5, but were not assigned apertures suitable for halo photometry in C5. A possible further extension of the present work would be to recover C5 light curves for these objects using either or both of smear or modified halo photometry.

Seven stars in Campaign 13 and one in Campaign 16 were not only assigned long-cadence halo apertures, but also downloaded at short cadence. For these targets we have provided both long and short cadence reductions. Following the analysis in Section 2 showing the insensitivity of short cadence CDPP to lags longer than ~ 100 cad and on choice of objective function, for consistency with long cadence we have adopted a 300 cadence lag (i.e. $30\times$ the long cadence lag of 10) and the L1 TV objective function. With their long timeseries the short cadence stars are computationally intractable for the Gaussian Process model in K2SC and we present otherwise uncalibrated halo lightcurves.

Analyses for several of the objects here have been previously published, but we here provide the first public data releases for the Pleiades' Seven Sisters (White et al. 2017), Aldebaran (Farr et al. 2018), ι Lib (Buysschaert et al. 2018), and ϵ Tau (Arentoft et al. 2019), as well as ρ Leo which was studied with halo pixels but without our objective functions (Aerts et al. 2018).

4. DISCUSSION

How well do we do? How do we quantify our lightcurve SNR?
Variability catalog?

The chemically-peculiar A0V star 98 Tau is of special interest for studies of surface inhomogeneity. We detect variability with a fundamental period of 1.74 d with twice as much power at the first harmonic ($P = 0.87$ d), which is consistent with α^2 CVn
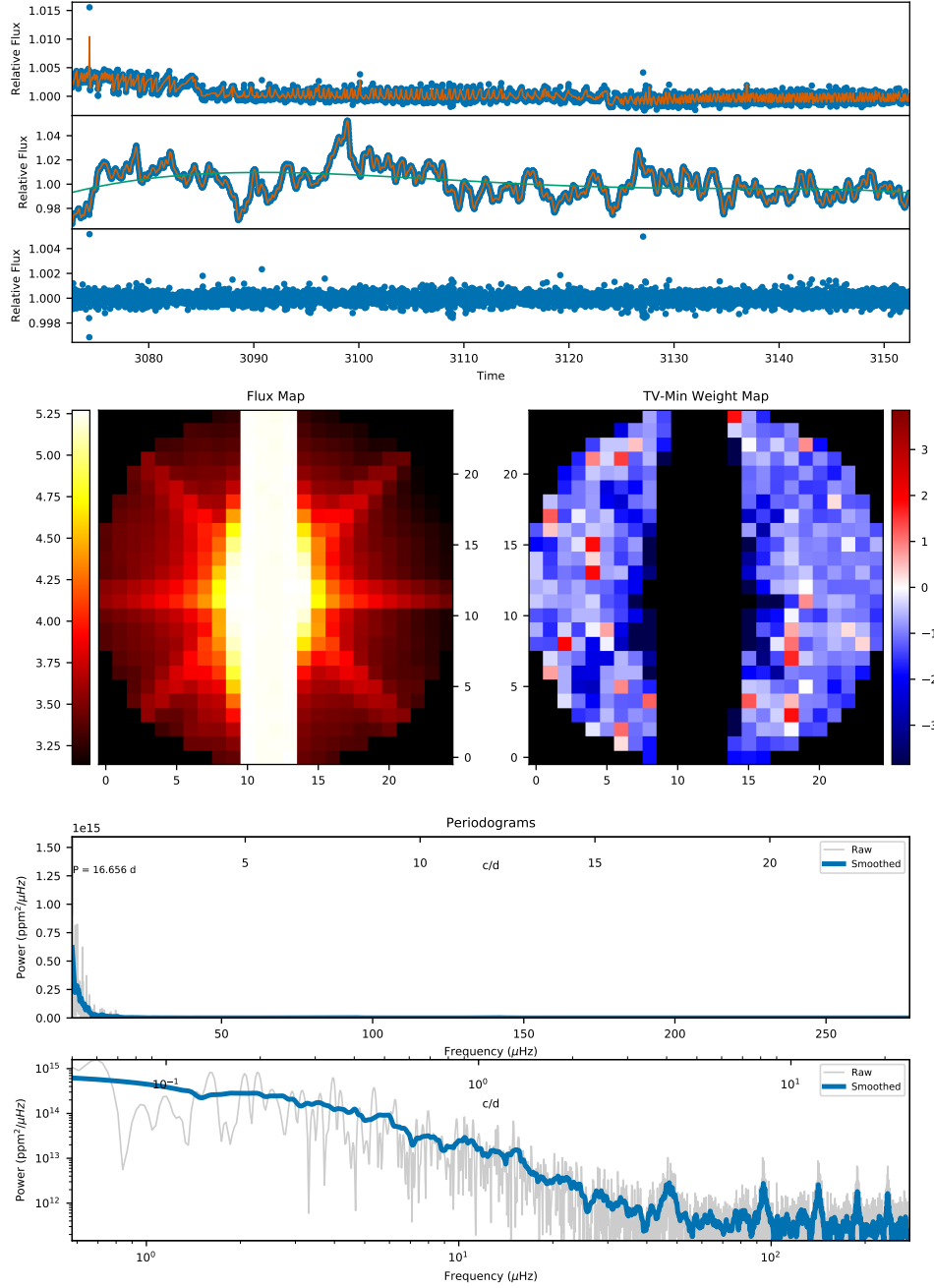
Figure 3. Summary plots for K2SC-corrected final halo light curve for ρ Leonis. The top three panels illustrate K2SC systematics correction: at the top, flux minus the GP time trend (blue dots) with GP x, y trend superimposed (orange line); in the middle, flux minus GP x, y components with GP time trend superimposed, and in green, a fifteenth-order polynomial trend; at the bottom the 'whitened' light curve with flux minus both GP components. Middle two panels: log-flux map (left) and halo log-weight map (right). Bottom two panels: periodograms in linear (top) and log (bottom) units of the residuals of the corrected light curve minus the long term polynomial trend. Plots of this form are available in supplementary online material for all long-cadence stars, together with similar plots for all short-cadence stars but without K2SC. The period at maximum power (16 d) is marked on all plots, though for ρ Leonis all variability is consistent with red noise (Bowman et al., 2019).

spot modulation from a rapidly-rotating star with a period of 1.74 d. This star also experiences a transit of depth 0.03, which for a 1.87 R$_\odot$ typical A0V star imply an 0.3 R$_\odot$ companion, almost certainly of stellar mass. With rotational modulation and an eclipse to break degeneracies, models such as `starry` (Luger et al. 2019) can infer surface brightness maps and reveal the spatial distribution of the star's chemical peculiarity.

5. CONCLUSIONS

Some of the objects presented here are the subject of more detailed work in preparation, namely Spica (Buzasi et al., in prep.) and the Hyades giants (White et al., in prep.). In addition to this, we aim to separately publish asteroseismic catalogues of the red giants (Yu et al., in prep.) and main-sequence stars (Greklek-McKeon et al., in prep.).

The sample of K2 bright stars presented here only includes those with halo apertures, but while some others are available conventionally, many were not assigned target pixels and were not downloaded at all. Smear photometry has been used to recover the brightest otherwise-unobserved stars in nominal *Kepler* (Pope et al., in prep.), and this can also be done in K2, although in the latter case the sample is much smaller due to competition with halo apertures and the systematics correction is more challenging. A natural extension of both pieces of work would be to produce smear light curves of all bright stars without halo apertures in K2, which would finally make the *Kepler* extended mission magnitude-complete at the bright end.

The halo method naturally extends to other contexts where simple aperture photometry is not possible, such as for saturated stars observed by the Transiting Exoplanet Survey Satellite (TESS; Ricker et al. 2015). Although the saturation limit is brighter ($T_{mag} \sim 6$) and this problem accordingly affects fewer stars and less badly, there are situations such as for α Centauri or β Hydri where the bleed column reaches the edge of the chip and a SAP light curve is irrecoverable. We expect that TV-min halo photometry will therefore be valuable in ensuring that TESS can observe even the very brightest stars.

ACKNOWLEDGEMENTS

This project was developed in part at the Building Early Science with TESS meeting, which took place in March 2019 at the University of Chicago.

REFERENCES

Aerts, C., Bowman, D. M., Símon-Díaz, S., et al. 2018, MNRAS, 476, 1234, doi: 10.1093/mnras/sty308

Aigrain, S., Hodgkin, S. T., Irwin, M. J., Lewis, J. R., & Roberts, S. J. 2015, MNRAS, 447, 2880, doi: 10.1093/mnras/stu2638

Aigrain, S., Parviainen, H., & Pope, B. J. S. 2016, MNRAS, 459, 2408, doi: 10.1093/mnras/stw706

Arentoft, T., Grundahl, F., White, T. R., et al. 2019, arXiv e-prints. https://arxiv.org/abs/1901.06187

Astropy Collaboration, Robitaille, T. P., Tollerud, E. J., et al. 2013, A&A, 558, A33, doi: 10.1051/0004-6361/201322068

Borucki, W. J., Koch, D., Basri, G., et al. 2010, Science, 327, 977, doi: 10.1126/science.1185402

Buysschaert, B., Neiner, C., Aerts, C., White, T. R., & Pope, B. J. S. 2018, in SF2A-2018: Proceedings of the Annual meeting of the French Society of Astronomy and Astrophysics, 369–372

Christiansen, J. L., Jenkins, J. M., Caldwell, D. A., et al. 2012, Publications of the Astronomical Society of the Pacific, 124, 1279, doi: 10.1086/668847

Farr, W. M., Pope, B. J. S., Davies, G. R., et al. 2018, ApJ, 865, L20, doi: 10.3847/2041-8213/aadfde

Foreman-Mackey, D., Hogg, D. W., & Morton, T. D. 2014, ApJ, 795, 64, doi: 10.1088/0004-637X/795/1/64

Fressin, F., Torres, G., Charbonneau, D., et al. 2013, ApJ, 766, 81, doi: 10.1088/0004-637X/766/2/81

Gilliland, R. L., Jenkins, J. M., Borucki, W. J., et al. 2010, ApJL, 713, L160, doi: 10.1088/2041-8205/713/2/L160

Guzik, J. A., Houdek, G., Chaplin, W. J., et al. 2016, ApJ, 831, 17, doi: 10.3847/0004-637X/831/1/17

Jones, E., Oliphant, T., Peterson, P., & Others. 2001, SciPy: Open source scientific tools for Python. http://www.scipy.org/

Kolenberg, K., Bryson, S., Szabó, R., et al. 2011, MNRAS, 411, 878, doi: 10.1111/j.1365-2966.2010.17728.x

Luger, R., Agol, E., Foreman-Mackey, D., et al. 2019, AJ, 157, 64, doi: 10.3847/1538-3881/aae8e5

Luger, R., Kruse, E., Foreman-Mackey, D., Agol, E., & Saunders, N. 2018, AJ, 156, 99, doi: 10.3847/1538-3881/aad230

Lund, M. N., Handberg, R., Davies, G. R., Chaplin, W. J., & Jones, C. D. 2015, ApJ, 806, 30, doi: 10.1088/0004-637X/806/1/30

Maclaurin, D., Duvenaud, D., & Adams, R. P. 2015, in ICML 2015 AutoML Workshop

Pérez, F., & Granger, B. E. 2007, Computing in Science and Engineering, 9, 21, doi: 10.1109/MCSE.2007.53

Petigura, E. A., Howard, A. W., & Marcy, G. W. 2013, Proceedings of the National Academy of Science, 110, 19273, doi: 10.1073/pnas.1319909110

Pope, B. J. S., White, T. R., Huber, D., et al. 2016, MNRAS, 455, L36, doi: 10.1093/mnrasl/slv143

Ricker, G. R., Winn, J. N., Vanderspek, R., et al. 2015, Journal of Astronomical Telescopes, Instruments, and Systems, 1, 014003, doi: 10.1117/1.JATIS.1.1.014003

Vinícius, Z., Barentsen, G., Hedges, C., & Gully-Santiago, M. 2018, KeplerGO/lightkurve: 1.0.0.dev1: First development release of lightkurve, doi: 10.5281/zenodo.1181929. https://doi.org/10.5281/zenodo.1181929

White, T. R., Huber, D., Maestro, V., et al. 2013, MNRAS, 433, 1262, doi: 10.1093/mnras/stt802

White, T. R., Pope, B. J. S., Antoci, V., et al. 2017, MNRAS, 471, 2882, doi: 10.1093/mnras/stx1050

Zhu, C., H. Byrd, R., & Lu, P. 1999

APPENDIX

Table 1. All stars observed with halo photometry in K2.

Name	EPIC	Spectral	V	Campaign	Comments
Alcyone	200007767	B7III	2.986	4	a
Atlas	200007768		3.763	4	a
Electra	200007769	B6IIIe	3.851	4	a
Merope	200007770	B6IVe	4.305	4	a
Maia	200007771	B8III	4.305	4	a
Taygeta	200007772	B6IV	4.448	4	a
Pleione	200007773	B8Vne	5.192	4	a
γ Tau	200007765	G9.5IIIabCN0.5	3.474	4	
δ1 Tau	200007766	G9.5IIICN0.5	3.585	4	
Spica	212573842	B1V	0.97	6, 17	No Halo Mask
69 Vir	212356048	K0III-IIIbCN1.5CH0.5	4.75	6	
Ascella	200062593	A2.5Va	2.585	7	
Albaldah	200062592	F2II-III	2.88	7	
τ Sgr	200062591	K1.5IIIb	3.31	7	
ξ2 Sgr	200062590	G8/K0II/III	3.51	7	
o Sgr	200062589	G9IIIb	3.77	7	
52 Sgr	200062585	B8/9V	4.598	7	
Ainalrami	200062588	K1II	4.845	7	
ψ Sgr	200062584	K0/1III+A/F	4.85	7	
43 Sgr	200062587	G8II-III	4.878	7	
ν2 Sgr	200062586	K3-II-III:CN1Ba1	4.98	7	
ϵ Psc	200068392	G9IIIbFe-2	4.28	8	
Revati	200068393	A7IV	5.187	8	
80 Psc	200068394	F2V	5.5	8	
42 Cet	200068399	G8IV+A(8)	5.87	8	
33 Cet	200068395	K4/5III	5.942	8	
60 Psc	200068396	G8III	5.961	8	
73 Psc	200068397	K5III	6.007	8	
WW Psc	200068398	M2.5III	6.14	8	
HR 243	200068400	G8/K0II/III	6.368	8	
HR 161	200068401	K3III	6.407	8	
HR 6766	200069361	G7:IIIbCN-1CH-3.5HK+1	4.56	9	
HR 6842	200069360	K3II	4.627	9	
4 Sgr	200069357	A0	4.724	9	
11 Sgr	200069358	K0III	4.98	9	
7 Sgr	200069362	F2II-III	5.34	9	

Table 1 *(continued)*

Name	EPIC	Spectral	V	Campaign	Comments
15 Sgr	200069359	O9.7Iab	5.37	9	
HR 6838	200069363	K2III	5.75	9	
Y Sgr	200069364	F8II	5.75	9	Cepheid
HR 6716	200069365	B0Iab/b	5.77	9	
HR 6681	200069366	A0V	5.929	9	
9 Sgr	200069368	O4V((f))z	5.97	9	
16 Sgr	200069367	O9.5III	6.02	9	
HR 6825	200069369	ApSi	6.15	9	
63 Oph	200069370	O8II((f))	6.2	9	
HR 6679	200069373	A1V	6.469	9	
HD 165784	200069371	A2Iab	6.58	9	
HD 161083	200069374	F0V	6.58	9	
5 Sgr	200069372	K0III	6.64	9	
HD 167576	200069378	K1III	6.66	9	
HR 6773	200069380	B3/5IV	6.71	9	
HD 163296	200071159	A1Vep	6.85	9	
HD 165052	200069379	O5.5:Vz+O8:V	6.87	9	
17 Sgr	200069375	G8/K0III	6.886	9	
HD 169966	200069376	G8/K0III	6.97	9	
HD 162030	200069377	K1III	7.02	9	
Porrima	200084004	F1V+F0mF2V	2.74	10	
Zaniah	200084005	A2IV	3.9	10	
21 Vir	200084006	B9V	5.48	10	
FW Vir	200084007	M3+IIICa0.5	5.71	10	
HR 4837	200084008	G8III	5.918	10	
HR 4591	200084009	K1III	6.316	10	
HR 4613	200084010	G8/K0III	6.364	10	
HD 107794	200084011	K0III	6.46	10	
θ Oph	200128906	OB	3.26	11	
44 Oph	200128907	kA5hA9mF1III	4.153	11	
45 Oph	200128908	F5III-IV	4.269	11	
51 Oph	200128909	A0V	4.81	11	
36 Oph	200129035	K2V+K1V	5.03	11	
o Oph	200128910		5.2	11	
26 Oph	200129034	F3V	5.731	11	
HR 6472	200128911	K0III	5.83	11	
HR 6366	200128913	Fm dD	5.911	11	
HR 6365	200128912	K0III	5.977	11	
191 Oph	200128914	K0III	6.171	11	

B. J. S. Pope et al.

Table 1 *(continued)*

Name	EPIC	Spectral	V	Campaign	Comments
κ Psc	200164167	A2VpSrCrSi	4.94	12	
83 Aqr	200164168	F0V	5.47	12	
24 Psc	200164169	K0II/III	5.94	12	
HR 8759	200164170	G5II/III	5.933	12	
14 Psc	200164171	A2II	5.87	12	
HR 8921	200164172	K4/5III	6.191	12	
81 Aqr	200164173	K4III	6.215	12	
HR 8897	200164174	K4III	6.34	12	
Aldebaran	200173843	K5+III	0.86	13	c
θ2 Tau	200173845	A7III	3.41	13	SC
ε Tau	200173844	G9.5IIICN0.5	3.53	13	d
θ1 Tau	200173846	G9IIIFe-0.5	3.84	13	
κ1 Tau	200173847	A7IV-V	4.201	13	SC
δ3 Tau	200173849	A2IV-Vs	4.25	13	C4
τ Tau	200173850	B3V	4.258	13	
υ Tau	200173848	A8Vn	4.282	13	SC
ρ Tau	200173851	A8V	4.65	13	SC
11 Ori	200173853	A1VpSiCr	4.661	13	
HR 1427	200173855	A6IV	4.764	13	SC
15 Ori	200173854	F2IV	4.82	13	
75 Tau	200173852	K1IIIb	4.969	13	
97 Tau	200173857	A7IV-V	5.085	13	SC
HR 1684	200173856	K5III	5.163	13	
κ2 Tau	200173859	F0Vn	5.264	13	SC
56 Tau	200173861	A0VpSi	5.346	13	
81 Tau	200173860	Am	5.454	13	
53 Tau	200173864	B9Vsp	5.482	13	
HR 1585	200173858	K1III	5.49	13	
80 Tau	200173866	F0V	5.552	13	
51 Tau	200173865	F0V	5.631	13	
HR 1403	200173867	Am	5.711	13	
89 Tau	200173868	F0V	5.776	13	
HR 1576	200173871	B9V	5.776	13	
98 Tau	200173870	A0V	5.785	13	
99 Tau	200173862	K0III	5.806	13	
105 Tau	200173869	B2Ve	5.92	13	
HR 1554	200173874	F2IVn	5.961	13	
HR 1385	200173875	F4V	5.965	13	C4
HR 1741	200173873	K0III	6.107	13	

Table 1 *(continued)*

Name	EPIC	Spectral	V	Campaign	Comments
HR 1633	200173872	K0	6.188	13	
HR 1755	200173876	K0III	6.205	13	
ρ Leo	200182931	B1Iab	3.87	14	e
58 Leo	200182925	K0.5IIIFe-0.5	4.838	14	
48 Leo	200182926	G8.5IIIFe-1	5.07	14	
53 Leo	200182928	A2V	5.312	14	
65 Leo	200182927	K0III	5.52	14	
35 Sex	200182929	K2II-III+K1II-III	5.79	14	
43 Leo	200182930	K3III	6.08	14	
Dschubba	200194910	B0.3IV	2.32	15	
Zubenelhakrabi	200194911	G8.5III	3.91	15	
ι1 Lib	200194912	B9IVpSi	4.54	15	b
41 Lib	200194913	G8III/IV	5.359	15	
ζ4 Lib	200194914	B3V	5.499	15	
HR 5762	200194915	A2IV	5.52	15	
HR 5806	200194916	K0III	5.79	15	
ζ3 Lib	200194917	K0III	5.806	15	
HR 5810	200194918	K0III	5.816	15	
ι2 Lib	200194919	A2V	6.066	15	b
HR 5620	200194920	K0III	6.14	15	
28 Lib	200194921	G8II/III	6.17	15	
HD 138810	200194958	K1(III)(+G)	7.02	15	
Asellus Australis	200200356	K0+IIIb	3.94	16	
Acubens	200200357	kA7VmF0/2III/IVSr	4.249	16	
ξ Cnc	200200358	G8.5IIIFe-0.5CH-1	5.149	16	
o1 Cnc	200200360	A5III	5.22	16	
η Cnc	200200359	K3III	5.325	16, 18	
45 Cnc	200200728	A3III:+G7III	5.65	16	SC
o2 Cnc	200200361	F0IV	5.677	16	
50 Cnc	200200363	A1Vp	5.885	16, 18	
82 Vir	200213053	M1+III	5.01	17	
76 Vir	200213054	G8III	5.21	17	
68 Vir	200213055	K5III	5.25	17	
80 Vir	200213056	K0III	5.706	17	
HR 5106	200213057	A0V	5.932	17	
HR 5059	200213058	A8V	5.965	17	
γ Cnc	200233186	A1IV	4.652	18	C5
ζ Cnc	200233643	F8V+G0V	4.67	18	C5
60 Cnc	200233188	K5III	5.44	18	C5, C16

Table 1 continued on next page

B. J. S. Pope et al.

Table 1 *(continued)*

Name	EPIC	Spectral	V	Campaign	Comments
49 Cnc	200233189	A1VpHgMnSiEu	5.66	18	C5
HR 3264	200233190	K1III	5.798	18	C5
29 Cnc	200233192	A5V	5.948	18	C5
HR 3222	200233193	G8III	6.047	18	C5
21 Cnc	200233196	M2III	6.08	18	C5
25 Cnc	200233644	F5IIIm?	6.1	18	C5
HR 3558	200233195	K1III	6.146	18	C5
HR 3541	200233194	C-N4.5	6.4	18	C5

[a]White et al. (2017)

[b]Buysschaert et al. (2018)

[c]Farr et al. (2018)

[d]Arentoft et al. (2019)

[e]Aerts et al. (2018)